TECHNICAL ARTICLE

Prediction and optimization of strain homogeneity in PTCAP process using ANFIS, ANN, and Taguchi approaches

Vahid Modanloo[1] · Behnam Akhoundi[1] · Ahmad Mashayekhi[1] · Hossein Talebi-Ghadikolaee[2]

Abstract

In this paper, the PTCAP (parallel tubular channel angular pressing) process as an SPD (severe plastic deformation) method is investigated. The effects of process parameters including channel angle, friction coefficient, and punch speed on strain homogeneity of the pure copper tube are studied. First, 9 experiments were designed by using Taguchi L9 orthogonal array. The experiments were carried out via the finite element method and the desired output was determined. The S/N (signal-to-noise) ratio and the ANOVA (analysis of variance) were used to determine the important parameters and calculate the contributions of each parameter. The results indicate that the channel angle has the most influence on strain homogeneity. In addition, a channel angle of 150 degrees, a friction coefficient of 0.05, and a punch speed of 9 mm/min led to the best result. Also, optimization results show almost a 6% improvement in strain homogeneity compared to conventional results. Finally, ANN (Artificial Neural Network) is used for predicting the output of the nine experiences. Afterwards, an ANFIS (Adaptive Neuro-Fuzzy Inference System) is also used for this prediction. Results show that the root square mean error in predicting the output using ANN is 5.51×10^{-3}, and it reduced magnificently to 7.39×10^{-7} using the benefits of fuzzy in ANFIS.

Keywords Severe plastic deformation · Simulation · Taguchi method · ANFIS · ANN

1 Introduction

Over recent years, many approaches have been applied to enhance the mechanical properties of metallic materials [1]. Ultra fine-grained (UFG) materials are extensively used in different industries because of their excellent mechanical properties [2]. The SPD (severe plastic deformation) technique is one of the most important methods for producing UFG materials [3]. There are some SPD methods to obtain high-strength metallic tubes such as HTCEE (hydrostatic tube cyclic expansion extrusion) [4], TCEC (tube cyclic extrusion compression) [5], HPTT (high-pressure tube twisting) [6], ASB (accumulative spin bonding) [7], TCP (tube channel pressing) [8], TCAP (tube channel angular pressing) [9], and PTCAP (parallel tubular channel angular pressing)

[10]. Among these approaches, PTCAP is an interesting process that has two important advantages compared with other processes, requiring lower loads and introducing better strain homogeneity across the tube thickness [11]. Figure 1 depicts the schematic of the PTCAP process [12]. In the first half cycle of this process, the first punch presses the tube into the two shear zones. Then, in the second half cycle, the second punch presses the tube back to its initial dimensions.

Faraji et al. [13] successfully applied the PTCAP process on pure copper tubes by experiment and FE simulation. They found that there is proper hardness homogeneity through the tube thickness and length direction. Also, there is a good agreement with the FE results. Afrasiab et al. [14] studied the effects of the multi-pass PTCAP on the microstructure and mechanical properties and also the outstanding energy absorption capacity of the PTCAPed Cu–Zn thin-walled tube. Severe anisotropy in UFG PTCAPed tubes compared with course-grained counterparts examined by Tavakkoli et al. [15]. Sanati et al. [16] evaluated the residual stress in UFG PTCAPed aluminum tubes via shearography. Faraji and Mousavi [17] numerically investigated the effect of process parameters like curvature and channel angles and deformation ratio in PTCAP process. Conventional methods for

✉ Vahid Modanloo
  v.modanloo@sirjantech.ac.ir

[1] Mechanical Engineering Department, Sirjan University of Technology, Sirjan, Iran

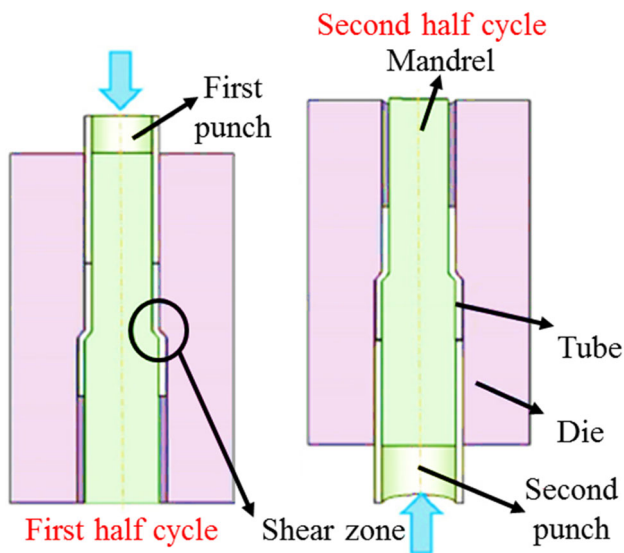[2] Faculty of Mechanical Engineering, University of Kashan, Kashan, Iran

Fig. 1 PTCAP process [12]

Table 1 Mechanical properties of pure copper [19]

Parameter	Value
Yield stress (MPa)	115
Young's modulus (GPa)	117
Density (kg/m^3)	8940
Poisson's ratio	0.32

Table 2 Input parameters with their levels

Parameter	Designation	Level		
		Low (1)	Medium (2)	High (3)
Channel angle (degree)	A	120	135	150
Friction coefficient	B	0.01	0.03	0.05
Punch speed (mm/min)	C	3	6	9

Table 3 Taguchi L9 orthogonal array

Trial no	Channel angle (degree)	Friction coefficient	Punch speed (mm/min)
1	120	0.01	3
2	120	0.03	6
3	120	0.05	9
4	135	0.01	6
5	135	0.03	9
6	135	0.05	3
7	150	0.01	9
8	150	0.03	3
9	150	0.05	6

engineering design are on the basis of trial and error or an experiment that causes an increase in time and cost. By combining optimization approaches with the DOE (design of experiments) and FE methods, cost-effective solutions can be obtained to attain favorable properties [18]. Despite the valuable works regarding the PTCAP, a DOE-based study was not found in the literature. In this paper, the effects of PTCAP process parameters i.e. channel angle, friction coefficient, and punch speed on strain homogeneity are investigated using the Taguchi DOE method.

2 Design and perform of experiments

The ABAQUS software was used for simulating the PTCAP process. A 2D model was used for the die set (punches, die, and mandrel) and tube. The length, outer diameter, and thickness of the tube are 40, 20, and 2.5 mm, respectively. The die set was modeled rigid body and the tube material was considered isotropic. The pure copper properties are given in Table 1 [19].

To define contact condition between the tube and the die set, the penalty contact interfaces was used. The tube was

modeled using CAX4R (axisymmetric four-node) element. The die set did not mesh since was modeled analytical rigid. Two steps were considered for accomplishing the PTCAP process. In the first step, the upper punch moves down with a fixed velocity of 0.05 mm/min to push the tube through the shear zone. In the second step, the lower punch goes up with the same velocity to reform the tube shape to its primary shape, while the upper punch is coming back. In both steps, the die and mandrel are fully fixed. Also, the Coulomb friction coefficient was assumed to be 0.05 [13]. Plastic strain homogeneity affects the internal microstructure homogeneity and as a result homogeneity in hardness measurements. Therefore, the SII (strain inhomogeneity index) was defined to calculate the strain inhomogeneity as follows:

$$SII = \frac{\varepsilon_{Max} - \varepsilon_{Min}}{\varepsilon_{Ave}} \tag{1}$$

where ε_{Max} and ε_{Min} are the maximum and minimum equivalent plastic strains, respectively. Also, ε_{Ave} indicates the average equivalent plastic strains along the processed tube thickness, [17]. Taguchi method is used in engineering analysis for optimizing the process [20]. The levels of the input parameters are given in Table 2. It should be noted that the parameter levels are selected based on the initial simulation
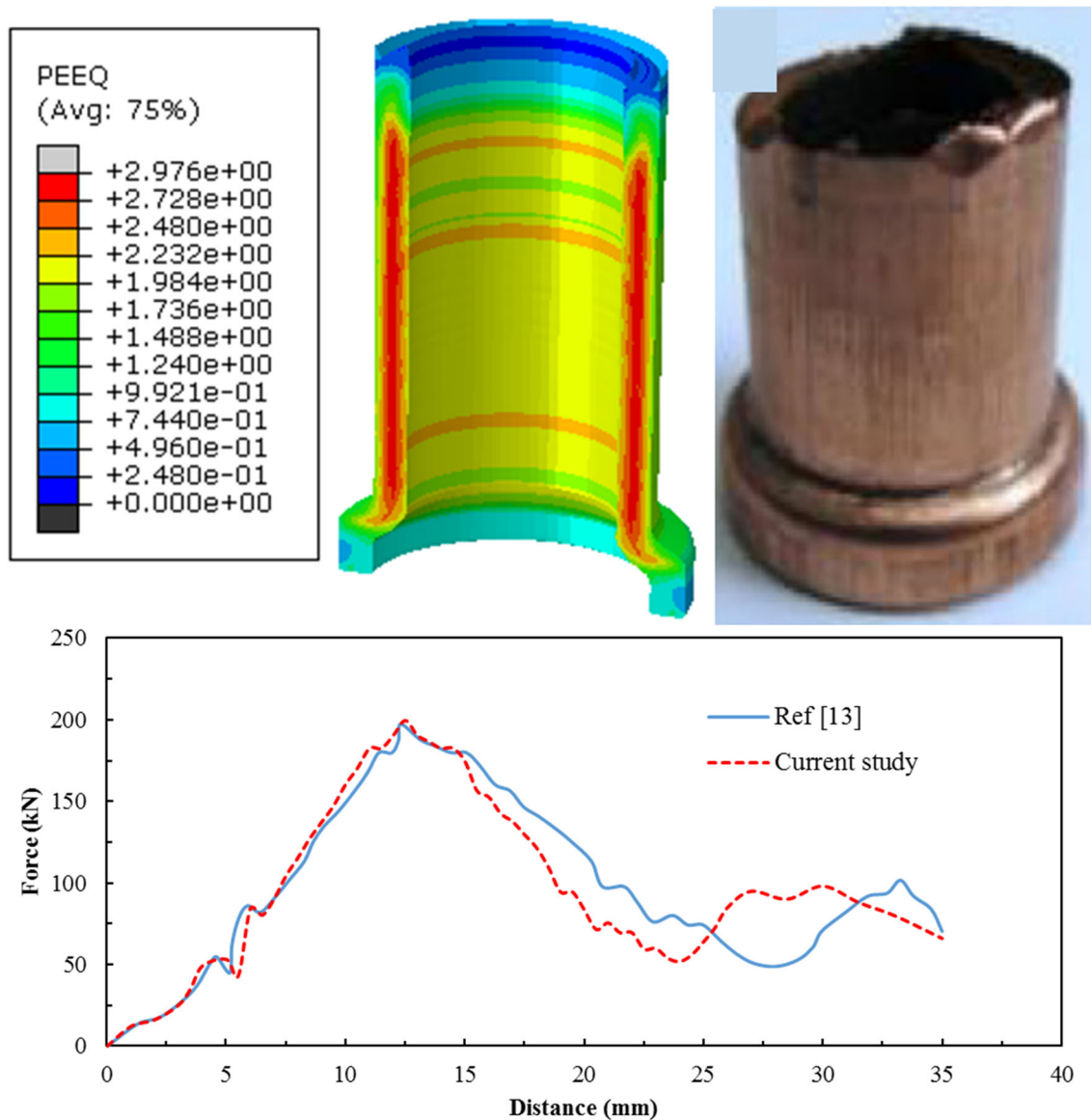
Fig. 2 Comparison of the PTCAPed tube and force–displacement curve of the current study with reference [13]

experiments. Table 3 presents the 9 experiments according to the Taguchi L9 orthogonal array. Minitab software was applied for data analyzing [21]. By considering three input parameters with three levels, totally 27 (3^3) runs are required and the Taguchi method suggests two experiment designs: L27 and L9. To save time, L9 orthogonal array was selected. In this study, lower SII shows better results. Therefore, "smaller is better" method was used in Taguchi approach to analyzing data as Eq. 2 [22]. Figure 2 shows the FE model of the PTCAP processed tube which is compared with the experiment of reference [13]. Moreover, the force–displacement curve of this reference is compared with current study that implies a good agreement between the results. In this FE experiment, the channel angle, friction coefficient, and punch speed are 120 degrees, 0.05, and 5 mm/min, respectively.

$$\frac{S}{N} = -10 \log \left(\frac{1}{n} \sum_{i=1}^{n} y_i^2 \right) \tag{2}$$

3 Design of ANFIS model

Adaptive Neuro-Fuzzy Inference System or Adaptive Network-based Fuzzy Inference System (ANFIS) is an adaptive and powerful combination of neural networks and fuzzy logic [23–25]. It is based on the Takagi–Sugeno inference systems of fuzzy, which is introduced in 1983 by Jang [26].
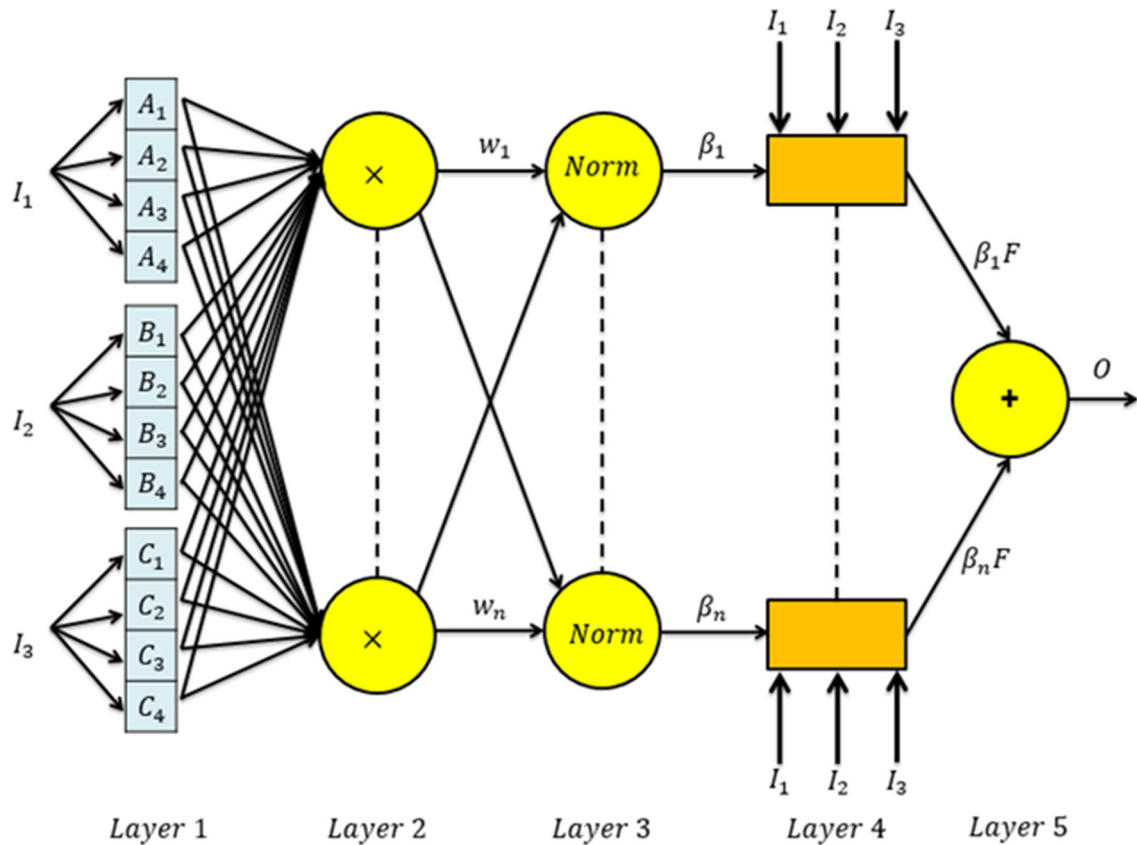
Fig. 3 A schematic view of Sugeno ANFIS model

Using both neural network and fuzzy, it has positive properties of both of these methods which makes it to be used in many applications such as [27–29]. An ANFIS uses a set of conditional IF–THEN rules which their property is modified using neural network; i.e., center of the membership functions, their starting and ending points are modified in an intelligent way using neural network. [30] It is composed of five different layers (as shown in Fig. 3.), described as follows:

- The first layer, defined as the "Input fuzzification layer" converts input values into a set of if-then fuzzy rules by using some membership functions (MFs). As an example, using a general bell-shaped MF for inputs, we can write Eqs. (3) to (5) for the first and the third input respectively.

$$\mu A_i(I_1) = \frac{1}{1 + \left[\left(\frac{I_1 - c_i}{a_i}\right)^2\right] \times b_i} \tag{3}$$

$$\mu B_i(I_2) = \frac{1}{1 + \left[\left(\frac{I_2 - c_i}{a_i}\right)^2\right] \times b_i} \tag{4}$$

$$\mu C_i(I_3) = \frac{1}{1 + \left[\left(\frac{I_3 - c_i}{a_i}\right)^2\right] \times b_i} \tag{5}$$

In the above equations μA_i, μB_i, and μC_i are the MFs of the input variables of I_1, I_2 and I_3, respectively. a_i, b_i and c_i parameters in the MFs belong to the interval of 0 to 1. These MFs are not constant and are changing according to the varying parameters.

- The second layer is responsible for creating power for rules. According to this task, this layer is defined as the "rule layer" and the output signal is calculated by multiplying the input signals with the fuzzy operators as follows:

$$w_i = \mu A_i(I_1) \times \mu B_i(I_2) \times \mu C_i(I_3); \; i = 1, \; 2, \; 3 \tag{6}$$

where w_i is the power of the fuzzy rule; thus, these nodes are called "rule nodes".

- In the third layer node power is calculated and normalized as the following equation for every neuron:

$$N_i = \frac{w_i}{\sum w_i}, \; i = 1, \; 2, \; 3, \; 4, \; ... \tag{7}$$

In fact, this layer normalizes the calculated power by dividing each value by the total power.

- In the fourth layer fuzzy quantities are de-fuzzified. Each node contains an adaptive node with a function, which yields representing fuzzy rules with combined MFs as follows:

$$N_i \times F_i = N_i \cdot (p_i \cdot (I_1) + q_i \cdot (I_2) + r_i I_3); \quad i = 1, 2, 3, ... \tag{8}$$

where N_i is the normalized node power, F_i is the fuzzy rule, p_i, q_i and r_i represents parameter set in each node.

- In the 5th layer output of the system is calculated based on sum of all incoming signals as the following equation:

$$O = \sum_i N_i \times F_i \tag{9}$$

4 Design of artificial neural network

Artificial neural network is a type of computer network that is inspired by the structure and functions of the human brain. Artificial neural networks are trained through a process called backpropagation, where the network learns from its mistakes and adjusts its connections between neurons accordingly. This allows the network to improve its performance over time and become more accurate in its predictions. Artificial neural networks have many benefits, such as their ability to process large amounts of data quickly, adapt to new information, and make complex decisions. However, they also have some disadvantages, such as being susceptible to bias and requiring a lot of computational power. Overall, they are a powerful tool in many industries and continue to advance and improve. It is used for pattern recognition, pharmaceutical research, water quality forecasting [31–33].

5 Results and discussion

Table 4 represents the results of 9 FE experiments based on the Taguchi L9 design. S/N ratio results of SII for the FE experiments are listed in Table 5. It is well known that among the levels of each parameter, the level with the highest S/N value is introduced as the optimal level [34]. Accordingly, the high level of all input parameters i.e. channel angle of 150 degrees, friction coefficient of 0.05, and punch speed of 9 mm/min are selected as the optimum condition (A3B3C3). Also, the main effects plot for means is demonstrated in Fig. 4. As can be interpreted from the S/N ratio results, channel angle is the most important factor for SII. Result shows that friction coefficient and punch speed have no remarkable

Table 4 Results of the SII

Experiment no	SII
1	0.50
2	0.37
3	0.33
4	0.56
5	0.52
6	0.50
7	0.36
8	0.32
9	0.31

Table 5 S/N ratio results of SII

Level	Channel angle (degree)	Friction coefficient	Punch speed (mm/min)
1	8.095	6.644	7.313
2	5.579	8.071	7.948
3	9.648	8.608	8.061
Delta	4.069	1.964	0.748
Rank	1	2	3

effect on the SII. Increasing channel angle causes a decrease in SII because, at larger channel angles, the material flow becomes more uniform and easier. As a result, a lower pressing load is required to complete the process. In other words, selecting higher channel angles is suitable from machine and energy consumption point of view [17]. Also, the effect of higher friction coefficient on the SII may be is attributed to the friction force and needs more investigation.

Figure 5 depicts the normal probability plot for the SII. As is shown, due to a P-Value of 0.69 (greater than 0.05), the data distribution is normal [35]. ANOVA results of SII are shown in Table 6. ANOVA results indicate that channel angle with 75.75% contribution is the most effective factor. On the other hand, the punch speed with a contribution of 2.75% is an almost ineffective factor. Also, the ANOVA model efficiency (R^2) was obtained equal to 96.50% which is desirable.

The predicted S/N ratio using the optimal parameters for SII is specified as A3B3C3 from S/N and ANOVA analysis. Table 7 compares the predicted SII and actual SII from the confirmation FE experiment. The initial parameters were chosen as A3B3C2 from the test number 9 in Table 4 in which the SII is minimum i.e. 0.31. The confirmation FE experiment shows that the S/N ratio improved almost by 0.6 dB from the initial parameters to optimal parameters, and SII increased by about 6%.
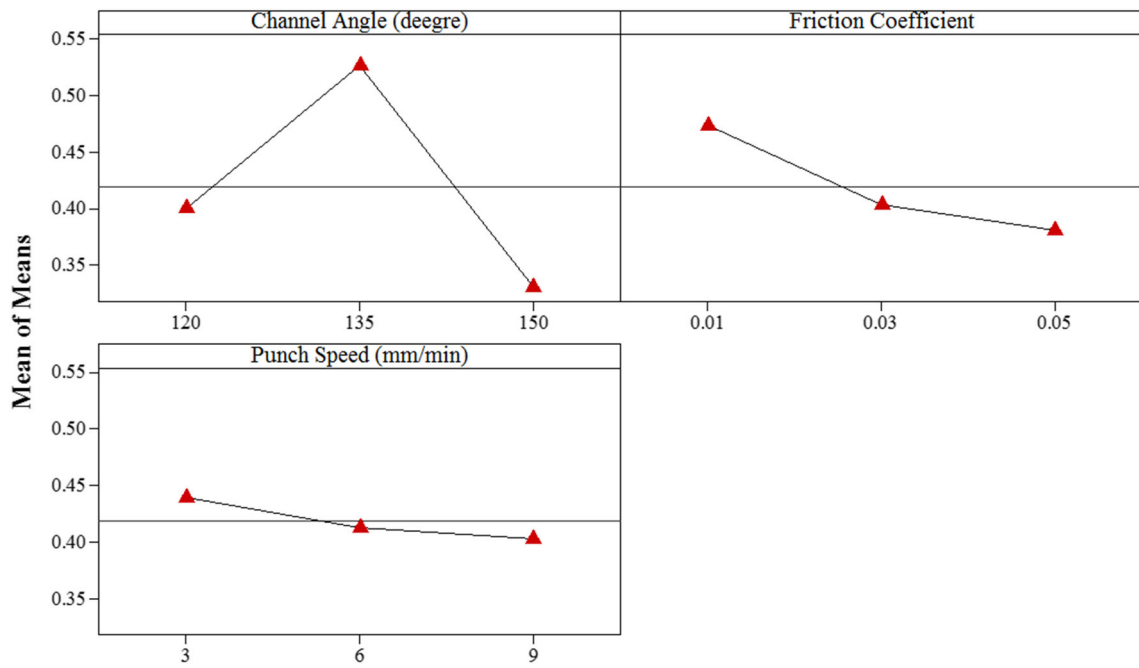
Fig. 4 Main effects plot for means of SII

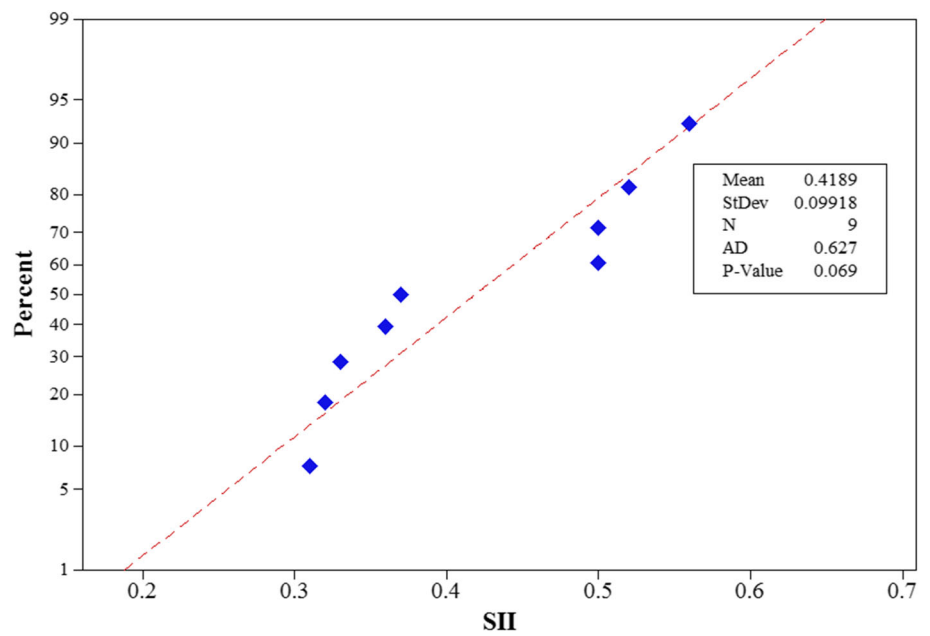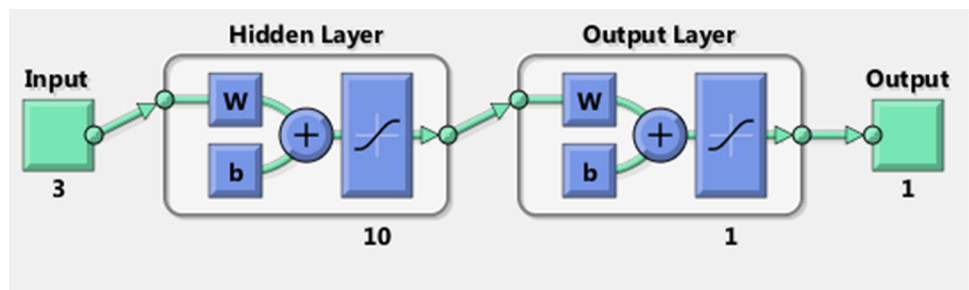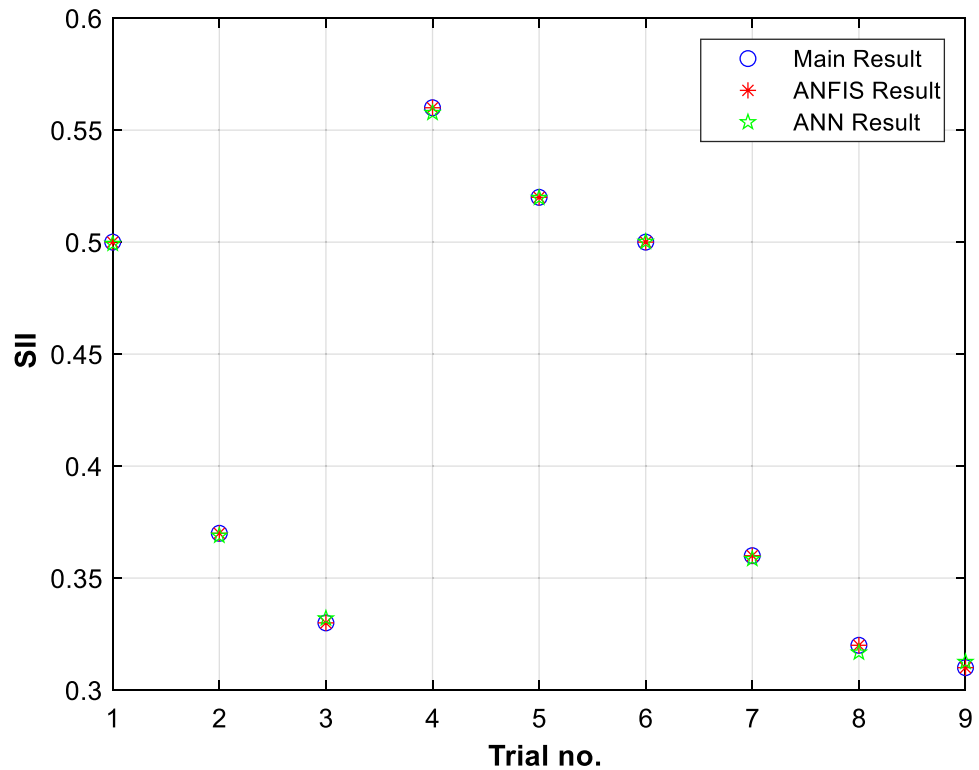**Fig. 5** Normal probability plot for SII

Fig. 6 Schematic view of the designed ANN

Fig. 7 Output of ANFIS vs main result

Table 6 ANOVA result of SII

Source	Sum square	Mean square	*P* value	Contribution (%)
Channel angle (deg)	0.059622	0.029811	0.044	75.75
Friction coefficient	0.014156	0.007078	0.163	18
Punch speed (mm/min)	0.002156	0.001078	0.561	2.75
Error	0.002756	0.001378	–	3.5
Total	0.078690	0.039345	–	100

Table 7 Results of the confirmation FE experiment

	Initial test	Optimal parameters	
		Prediction	FE Test
Parameter levels	A3B3C2	A3B3C3	A3B3C3
SII	0.31	0.28	0.29
Calculated S/N ratio	10.1728	10.7686	10.7520

In this paper, ANN and ANFIS are also used for training and predicting the desired output. For this purpose, three parameters of channel angle, friction coefficient, and punch speed are considered as input parameters with values mentioned in Table 3; also output is the SII as reported in Table 4. While using ANN, the three mentioned inputs goes to a hidden layer consists of 10 neurons. Each neuron has some weights (bias and gain) which will be determined in such a way that ANN can predict the output more precisely. An output layer creates the final output (as depicted in Fig. 6).

In the ANFIS, the MFs are assumed to be Gaussian type, with three membership functions for each input. The ANIS

model has 78 nodes, 27 linear parameters, 18 nonlinear parameters, 9 training data pairs, and 27 fuzzy rules. After 10 epochs of training, ANFIS can fit itself with the experimental data very well. Training data versus the output of the ANN and ANFIS are compared in Fig. 7. According to this figure, it is clear that ANN and ANFIS are capable of predicting the output accurately. More precise analysis shows that the RSME in predicting the outputs using ANN is 5.51×10^{-3}, while using ANFIS it reduced to 7.39×10^{-7} in ANFIS due to using neural-network and fuzzy logic simultaneously. Surfaces of the output (SII) versus each pair of the inputs are shown in Figs. 8, 9 and 10. As mentioned before (see Table 6), channel angle and friction coefficient are the most important parameters on the SII. Hence, in Fig. 8 when the friction coefficient goes near the 0.03, the SII increases.
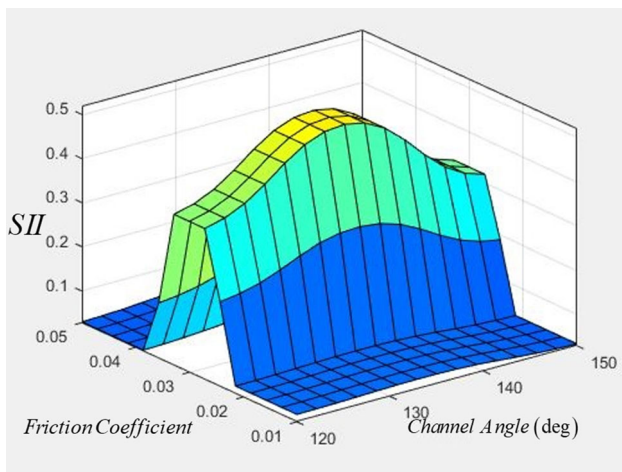
Fig. 8 Surface of the SII versus channel angle and friction coefficient
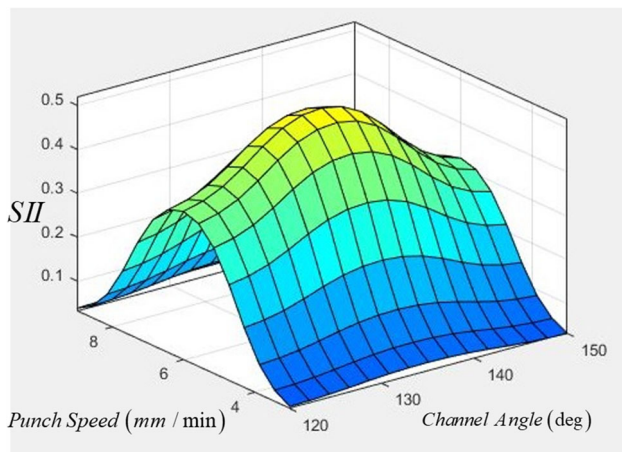

Fig. 10 Surface of the SII versus friction coefficient and punch speed

Fig. 9 Surface of the SII versus channel angle and punch speed

3. The used ANN and ANFIS models could predict the outputs (strain homogeneity index) with high accuracy, while the ANFIS had more precision.

Declarations

Conflict of interest The authors declare that they have no conflict of interest.

6 Conclusions

In this paper, process parameters optimization of the PTCAP has been investigated using the design of experiments and finite element approaches. Taguchi L9 orthogonal array was used for designing the required experiments by combination of channel angle, friction coefficient, and punch speed as input parameters. The main results of the research are summarized as follow:

1. The channel angle with a contribution of 75.75% is the most important factor compared to the friction coefficient (a contribution of 18%) and the punch speed (a contribution of 2.75%) on the strain homogeneity of the PTCAPed pure copper tube.
2. The confirmation experiment showed almost a 6% improvement in strain homogeneity compared with the conventional results.
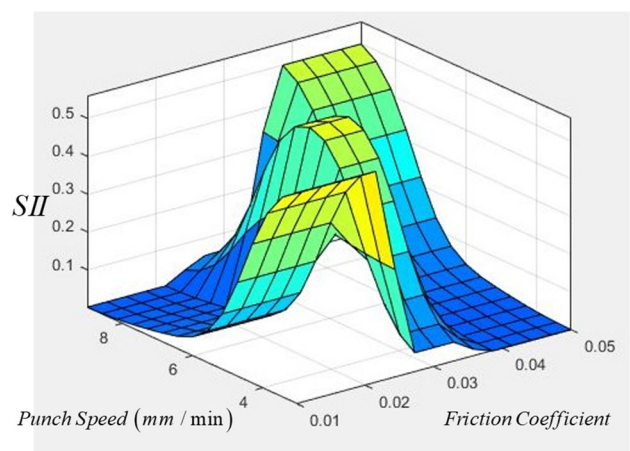
References

1. Siahsarani, A., Samadpour, F., Mortazavi, M.H., Faraji, G.: Microstructural, mechanical and corrosion properties of AZ91 magnesium alloy processed by a severe plastic deformation method of hydrostatic cyclic expansion extrusion. Met. Mater. Int. **27**, 2933–2946 (2021)
2. Hosseini, S.M., Roostaei, M., Mosavi Mashhadi, M., Jabbari, H., Faraji, G.: Fabrication of al/mg bimetallic thin-walled ultrafine-grained tube by severe plastic deformation. J. Mater. Eng. Perform. **31**(5), 4098–4107 (2022)
3. Bodkhe, M., Sharma, S., Mourad, A.H.I., Babu Sharma, P.: A review on SPD processes used to produce ultrafine-grained and multilayer nanostructured tubes. Mater. Today Proc. **46**, 8602–8608 (2021)
4. Savarabadi, M.M., Faraji, G., Zalnezhad, E.: Hydrostatic tube cyclic expansion extrusion (HTCEE) as a new severe plastic deformation method for producing long nanostructured tubes. J. Alloy. Compd. **785**, 163–168 (2019)
5. Babaei, A., Mashhadi, M.M., Jafarzadeh, H.: Tube cyclic extrusion compression (TCEC) as a novel severe plastic deformation method for cylindrical tubes. Mater. Sci. Eng. A **598**, 1–6 (2014)
6. Toth, L.S., Chen, C., Pougis, A., Arzaghi, M., Fundenberger, J.J., Mansion, R., Suwas, S.: High pressure tube twisting for producing ultra-fine grained materials: a review. Mater. Trans. **60**(7), 1177–1191 (2019)
7. Mohebbi, M.S., Akbarzadeh, A.: Accumulative spin bonding (ASB) as a novel SPD process for fabrication of nanostructured tubes. Mater. Sci. Eng. A **528**(1), 180–188 (2010)

8. Farshidi, M.H., Rifai, M., Miyamoto, H.: Grain refinement, texture evolutions, and strengthening of a recycled aluminium alloy subjected to tube channel pressing. Kovove Mater. **61**, 13–21 (2023)

9. Kunčická, L., Kocich, R., Ryukhtin, V., Cullen, J.C., Lavery, N.P.: Study of structure of naturally aged aluminium after twist channel angular pressing. Mater Charact **152**, 94–100 (2019)

10. Abd El Aal, M.I., Gadallah, E.A.: Parallel tubular channel angular pressing (PTCAP) processing of the Cu-20.7 Zn-2Al tube. Materials **15**(4), 1469 (2022)

11. Abd El Aal, M.I., El-Fahhar, H.H., Mohamed, A.Y., Gadallah, E.A.: Influence of parallel tubular channel angular pressing (PTCAP) processing on the microstructure evolution and wear characteristics of copper and brass tubes. Materials **15**(9), 2985 (2022)

12. Hosseini, A., Rahmatabadi, D., Hashemi, R., Akbari, H.: Experimental and numerical assessment of energy absorption capacity of thin-walled Al 5083 tube produced by PTCAP process. Trans. Nonferrous Metals Soc. China **30**(5), 1238–1248 (2020)

13. Faraji, G., Babaei, A., Mashhadi, M.M., Abrinia, K.: Parallel tubular channel angular pressing (PTCAP) as a new severe plastic deformation method for cylindrical tubes. Mater. Lett. **77**, 82–85 (2012)

14. Afrasiab, M., Faraji, G., Tavakkoli, V., Mashhadi, M.M., Dehghani, K.: The effects of the multi-pass parallel tubular channel angular pressing on the microstructure and mechanical properties of the Cu-Zn Tubes. Trans. Indian Inst. Metals **68**(5), 873–879 (2015)

15. Tavakkoli, V., Afrasiab, M., Faraji, G., Mashhadi, M.M.: Severe mechanical anisotropy of high-strength ultrafine grained Cu-Zn tubes processed by parallel tubular channel angular pressing (PTCAP). Mater. Sci. Eng. A **625**, 50–55 (2015)

16. Sanati, H., Reshafi, F., Faraji, G., Soltani, N., Zalnezhad, E.: Evaluation of residual stress in ultrafine-grained aluminum tubes using shearography. Proc. Inst. Mech. Eng. Part B J. Eng. Manuf. **229**(6), 953–962 (2015)

17. Faraji, G., Mashhadi, M.M.: Plastic deformation analysis in parallel tubular channel angular pressing (PTCAP). J. Adv. Mater. Process. **1**(4), 23–32 (2013)

18. Alimirzaloo, V., Modanloo, V.: Minimization of the sheet thinning in hydraulic deep drawing process using response surface methodology and finite element method. Int. J. Eng. Trans. B Appl. **29**(2), 264–273 (2016)

19. Modanloo, V., Gorji, A., Bakhshi-Jooybari, M.: Effects of forming media on hydrodynamic deep drawing. J. Mech. Sci. Technol. **30**(5), 2237–2242 (2016)

20. Modanloo, V., Gorji, A., Bakhshi-Jooybari, M.: A comprehensive thinning analysis for hydrodynamic deep drawing assisted by radial pressure. Iran. J. Sci. Technol. Trans. Mech. Eng. **43**, 487–494 (2019)

21. Babazadeh Asbagh, E., Modanloo, V., Alimirzaloo, V., Donyavi, A.: Experimental investigation of the effect of process parameters on the surface roughness in finishing process of chrome coated printing cylinders. Int. J. Eng. Trans. C Asp. **29**(12), 1775–1782 (2016)

22. Moradian, M., Doniavi, A., Modanloo, V., Alimirzaloo, V.: Process parameters optimization in gas blow forming of pin-type metal bipolar plates using Taguchi and finite element methods. ADMT J. **10**(2), 101–108 (2017)

23. Hemalatha, A., Reddy, V.D., Prasad, K.: Evolution of regression and ANFIS models for wire spark erosion machining of aluminium metal matrix composites for aerospace applications. Int. J. Interact. Des. Manuf. (2022). https://doi.org/10.1007/s12008-022-01012-x

24. Singh, J.: Multi-objective optimization of powder-mixed EDM parameters using hybrid Grey-ANFIS artificial intelligence technique. Int. J. Interact. Des. Manuf. **16**, 1533–1549 (2022)

25. Goyal, A., Sharma, D., Bhowmick, A., et al.: Experimental investigation for minimizing circularity and surface roughness under nano graphene mixed dielectric EDM exercising fuzzy-ANFIS approach. Int. J. Interact. Des. Manuf. **16**, 1135–1154 (2022)

26. Rao, T.B.: Prediction of EDMed micro-hole quality characteristics using hybrid bio-inspired machine learning-based predictive approaches. Int. J. Interact. Des. Manuf. **17**, 747–764 (2023)

27. Saifan, A., Chen, S., Saifan, S., et al.: Seam tracking control for weld cladding of boiler tubes in thermal power plants. Int. J. Interact. Des. Manuf. **18**, 1709 (2023)

28. Sukonna, R.T., Zaman, P.B., Dhar, N.R.: Estimation of machining responses in hard turning under dry and HPC conditions using different AI based and statistical techniques. Int. J. Interact. Des. Manuf. **16**, 1705–1725 (2022)

29. Prashanth, P., Hiremath, S.S.: Experimental and predictive modelling in dry micro-drilling of titanium alloy using Ti–Al–N coated carbide tools. Int. J. Interact. Des. Manuf. **17**, 553–577 (2023)

30. Thejasree, P., Natarajan, M.: Applications of hybrid artificial intelligence tool in wire electro discharge machining of 7075 aluminium alloy. Int. J. Interact. Des. Manuf. (2023). https://doi.org/10.1007/s12008-023-01315-7

31. Abiodun, O.I., Jantan, A., Omolara, A.E., Dada, K.V., Umar, A.M., Linus, O.U., Arshad, H., Kazaure, A.A., Gana, U., Kiru, M.U.: Comprehensive review of artificial neural network applications to pattern recognition. IEEE Access. **4**(7), 158820–158846 (2019)

32. Agatonovic-Kustrin, S., Beresford, R.: Basic concepts of artificial neural network (ANN) modeling and its application in pharmaceutical research. J. Pharm. Biomed. Anal. **22**(5), 717–727 (2000)

33. Palani, S., Liong, S.Y., Tkalich, P.: An ANN application for water quality forecasting. Mar. Pollut. Bull. **56**(9), 1586–1597 (2008)

34. Modanloo, V., Hasanzadeh, R., Esmaili, P.: The study of deep drawing of brass-steel laminated sheet composite using taguchi method. Int. J. Eng. Trans. A Basics **29**(1), 103–108 (2016)

35. Modanloo, V., Alimirzaloo, V.: Investigation of the forming force in torsion extrusion process of aluminum alloy 1050. Int. J. Eng. Trans. C Asp. **30**(6), 920–925 (2017)